THE JOURNAL OF PHYSICAL CHEMISTRY Letters

Letter

pubs.acs.org/JPCL

Theory of Light-Modulated Emission Spectroscopy

Mehdi Ansari-Rad*,† and Juan Bisquert*,‡

†Department of Physics, Shahrood University of Technology, Shahrood, Iran

‡Institute of Advanced Materials (INAM), Universitat Jaume I, 12006 Castelló, Spain

Supporting Information

ABSTRACT: Perovskite solar cells and fluorescent collectors formed by a dispersion of quantum dots in a transparent solid are paradigmatic devices for photon capture and utilization that involve the coupling of photon displacement, absorption and regeneration. In order to obtain information about the coupled photonic processes in systems involving photon recycling, we analyze the transfer function for modulated outgoing to incoming photon flux. We show the physical features of light-to-light impedance that reveals a trap-limited diffusion of photons coupled with the nonradiative recombination. The spectral shapes allow one to distinguish readily photonic recombination and diffusion kinetic phenomena and consequently to determine the physical parameters that control the system's quantum yield for photoluminescence.

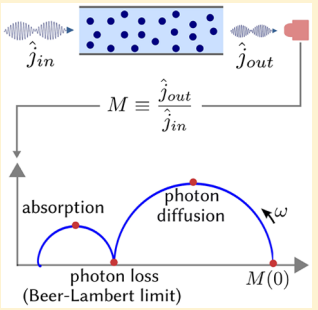

Frequency domain methods are central tools for the characterization of semiconductor materials and solar cells. The most widely used technique is the electrical impedance spectroscopy, where a modulated current output is measured with respect to voltage input.[1] This method has the unique ability to separate conduction and polarization processes that oscillate at separated characteristic frequencies and provides a wealth of information about materials and device operation. For optically active materials and devices, especially in nanostructured solar cells, light-to-electrical modulated techniques have been used for many years.[2−4] Recently a generalization has been presented that unifies the calculation of any modulated transfer function on the basis of the three main experimental axes: voltage, electrical current, and illumination flux incident on the device.[5]

In the previous report, however, we have not covered the modulation of outgoing to incoming light, which appears an excellent tool for the exploration of luminescent and fluorescent materials. In fact, light-to-light modulated techniques are important and straightforward methods for the determination of decay lifetimes in molecules[6] and recombination lifetimes in semiconductors.[7] However, it has been widely recognized that the unrivalled power of modulated techniques appears in systems where several local and spatially distributed phenomena become entangled, as in diffusion coupled with trapping and recombination.[8,9]

Here we describe the application of light-modulated emission spectroscopy (LIMES) to a new class of photonic systems with strong internal coupling of matter and radiation. For example in fluorescent collectors composed of organic dyes or inorganic quantum dots embedded in a transparent framework, a large photon density is created by absorption and reemission that is finally expelled at one side of the slab.[10,11] When the electronic quality of solar cells becomes proficient, as in GaAs solar cells and more recently in lead halide perovskite solar cells, the optical properties of the device take a leading role for obtaining high energy conversion efficiency. Internal photon absorption and reemission are coupled with the mobile concentrations of electrons and holes that form the recombination centers, in the phenomena termed photon recycling that exerts a significant impact on solar cell efficiency.[12−14]

Here we formulate an untrivial model of the frequency modulated luminescence, considering fixed absorption-recombination centers as in a fluorescent collector, although the extension with the coupling to mobile carriers[13] is straightforward. We analyze the response of an absorbing layer of thickness d, intrinsic absorption coefficient α, and refractive index n_r to an external modulated monochromatic illumination. Absorption of the photons in the absorbing layer mainly occurs via the fluorescent centers, for example dye molecules or quantum dots, that are homogeneously dispersed in the layer. Therefore, we introduce another absorption coefficient α' that is related to the number density of the absorbing centers and their absorption cross section, so that $\alpha' \gg \alpha$.

As schematically shown in Figure 1, a photon with a frequency ν_0, after being absorbed by an absorber, is either reemitted isotropically or lost nonradiatively, with the rates ϵ and κ, respectively. Therefore, at any time t, we can distinguish between two types of photons in the layer, the photons that freely travel in the system, and those that are trapped by the fluorescent centers. Note that the radiative processes may result in another population of the photons, with frequency $\nu < \nu_0$, in the system, due to Stoke's shift. But in the following we consider only the population of the original photons, that is, those that are injected into the system by an external source, which can be absorbed and reemitted in internal recycling. In

Received: June 19, 2017
Accepted: July 21, 2017
Published: July 21, 2017

DOI: 10.1021/acs.jpclett.7b01563
J. Phys. Chem. Lett. 2017, 8, 3673−3677

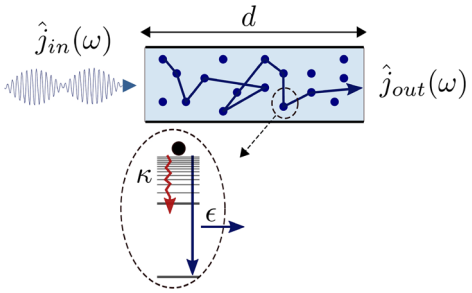

Figure 1. Schematic illustration showing a layer with thickness d homogeneously doped with fluorescent absorbing centers (filled circles in the layer). At $x = 0$, the layer is illuminated with an external source, leading to a flux of photons into the layer at $x = 0$ and an outgoing flux at $x = d$. $\hat{j}_{in}(\omega)$ is a small sinusoidal perturbation of the external illumination superimposed to the steady state (not shown) and $\hat{j}_{out}(\omega)$ is the corresponding outgoing photon flux. κ and ϵ are the rate constant of nonradiative and radiative decay, respectively. Filled circle in the bottom shows electron of an excited absorbing center going back to its ground state.

fact, κ is treated as a cumulative rate constant that accounts for all mechanisms that lead to irreversible loss of the original photon. We also define lifetime of the photon (the average time between two successive absorption events) as the inverse of the absorption rate constant $\beta = c\alpha'$, where c is the speed of light in the medium. Using these definitions, the continuity equations for the trapped and free photons read

$$\frac{\partial \gamma^{t}}{\partial t} = \beta\gamma^{f} - \epsilon\gamma^{t} - \kappa\gamma^{t} \tag{1}$$

$$\frac{\partial \gamma^{f}}{\partial t} = -\frac{\partial j}{\partial x} + (\epsilon\gamma^{t} - \beta\gamma^{f}) \tag{2}$$

where $\gamma^{f(t)}$ is the number density of the free (trapped) photons per energy interval, and $j = -D\partial\gamma^{f}/\partial x$ is the photon flux in the layer with $D = c/\alpha$ being the photon diffusion coefficient. The term in the parentheses in eq 2 is in fact the net rate of the free photon generation in a macroscopic volume element. To establish a connection between the absorption and emission rate constants, that is β and ϵ, let us neglect the nonradiative loss term in eq 1 and consider the equilibrium conditions in the absence of the incoming external illumination. In these conditions, eq 1 implies that $\beta\gamma_0^{f} = \epsilon\gamma_0^{t}$, where the subscript indicates the zero illumination. On the other hand, since the equilibrium population of the photons at temperature T is determined by the corresponding blackbody spectrum, one can write $\gamma_0^{f} = \gamma_{bb}(T)$. Therefore, we get

$$\epsilon = \beta\frac{\gamma_{bb}(T)}{\gamma_0^{t}} \tag{3}$$

We note that γ_0^{t} is itself proportional to the density of states of the fluorescent material. eq 3 is an important relation because it can be used to find an estimation for the typical values of the emission rate constant in terms of the intrinsic properties of the absorbing centers and the equilibrium radiation field.

To complete the continuity equations, we consider the simple 1D model depicted in Figure 1 and adopt the following boundary conditions

$$j_{(x=0)} = j_{in} \tag{4}$$

$$j_{(x=d)} = j_{out} = S \times (\gamma^{f}_{(x=d)} - \gamma^{f}_{0}) \tag{5}$$

The first boundary condition describes injection of photons by an external illumination into the layer. The second equation describes a partially reflecting boundary condition, where we have introduced a velocity S that controls the strength of the emissivity of the layer at $x = d$.

Under steady state external illumination, all quantities j_{in}, j_{out}, γ^{f}, and γ^{t} are time-independent. But let us consider the effect of a small sinusoidal perturbation of the external illumination, $\hat{j}_{in}(\omega)$, superimposed to the steady state (note that ω is used for the angular frequency of the modulation). As a consequence of this small perturbation, a change in the photon population as $\hat{\gamma}(\omega)$ occurs in the layer that, in turn, results in a modulated change in the outgoing flux, $\hat{j}_{out}(\omega)$. For the small perturbation variables, we use the Laplace transform of linearized eqs 1 and 2 that can be done by the substitution $\partial/\partial t \rightarrow i\omega$, where $i = \sqrt{-1}$. The result is

$$i\omega\hat{\gamma}^{t} = \beta\hat{\gamma}^{f} - \epsilon\hat{\gamma}^{t} - \kappa\hat{\gamma}^{t} \tag{6}$$

$$i\omega\hat{\gamma}^{f} = -\frac{\partial \hat{j}}{\partial x} + \epsilon\hat{\gamma}^{t} - \beta\hat{\gamma}^{f} \tag{7}$$

which now have to be solved with the transformed boundary conditions

$$\hat{j}_{(x=0)} = \hat{j}_{in} \tag{8}$$

$$\hat{j}_{(x=d)} \equiv \hat{j}_{out} = S\hat{\gamma}^{f}_{(x=d)} \tag{9}$$

By solving eq 6 for $\hat{\gamma}^{t}$ and substituting it in eq 7, we obtain the following equation for the free photon population

$$\frac{\partial^2\hat{\gamma}^{f}}{\partial x^2} - \frac{1}{l^2}\hat{\gamma}^{f} = 0 \tag{10}$$

where

$$\frac{1}{l^2(\omega)} = \alpha\alpha'\left(i\frac{\omega}{\beta} + \frac{i\omega + \kappa}{i\omega + \epsilon + \kappa}\right) \tag{11}$$

Now, in analogy with the concepts in the traditional impedance spectroscopy, we define a light-to-light transfer function as

$$M(\omega) = \frac{\hat{j}_{out}(\omega)}{\hat{j}_{in}(\omega)} \tag{12}$$

which is, in fact, a modulated quantum yield. $M(\omega)$ can straightforwardly be obtained by solving the small perturbation equations with the corresponding boundary conditions. By doing this, we get

$$M(\omega) = \frac{1}{\left(\frac{D}{Sl}\right)\sinh(d/l) + \cosh(d/l)} \tag{13}$$

The transfer function can be written as $M(\omega) = M'(\omega) - iM''(\omega)$, where M' and M'' are the real and imaginary parts of the transfer function, respectively.

As mentioned above, we neglect in this model the downshift of frequencies, which is usually a good approximation for fluorescent collectors. However, the detailed spectral properties of the absorption and reemission could be evaluated by well-known methods.[10,15,16] The modulated response could be established for arbitrary incoming and outgoing wavelength,

DOI: 10.1021/acs.jpclett.7b01563
J. Phys. Chem. Lett. 2017, 8, 3673−3677

leading generalized light-impedance functions. Although this topic is outside the scope of the present work, we have shown in the SI that the downshift of frequencies does not change the transfer function obtained in eq 13.

Let us before presenting our results for the transfer function over a broad modulation frequency range, consider the static regime, that is, $\omega \to 0$, where the transfer function is the derivative of the external quantum efficiency for photoluminescence, $M(0) = \mathrm{d}j_{out}/\mathrm{d}j_{in}$.[5] To obtain some insights into the interpretation of $M(0)$, we examine two limiting cases of $\epsilon \gg \kappa$ and $\epsilon \ll \kappa$, equivalent to $l \to \infty$ and $l \to 1/\sqrt{\alpha\alpha'}$, respectively. These are in fact high and low fluorescence quantum yield regimes. It is found that

$$M(0) \approx \begin{cases} \dfrac{2}{1+\sqrt{\alpha'/\alpha}} e^{-d\sqrt{\alpha\alpha'}} & \epsilon \ll \kappa \\ 1 & \epsilon \gg \kappa \end{cases} \tag{14}$$

By choosing $\alpha = \alpha'$, one can see that the first case is in fact the well-known Beer–Lambert law (note that for the derivation, we furthermore assumed a very good emissivity as $S = c$; see also below). In this case, each absorbed photon is lost by a nonradiative decay process. It is interesting that our model which is based on a random walk picture of the photon transport can show how and when the Beer–Lambert law is satisfied. On the other hand, if $\epsilon \gg \kappa$, as we expect, the transfer function is unity because there are no losses in the system and every injected photon into the layer is finally extracted from it. This response is different from the traditional Beer–Lambert law and is closely related to the photon recycling concept.

In order to study the frequency dependence of the transfer function $M(\omega)$, we introduce two characteristic frequencies as below

$$\omega_\beta = \beta \tag{15}$$

$$\omega_{D'} = \frac{\epsilon}{d^2\alpha\alpha'} \tag{16}$$

We note that $\omega_{D'}$ is the characteristic frequency of diffusion in a finite layer of thickness d with an effective diffusion coefficient of $D' = D\epsilon/\beta$. Although the diffusion coefficient of the free photons is given by $D = c/\alpha$, it is reduced by a factor of ϵ/β as a result of the trapping events (absorption of photons by the fluorescent centers). Therefore, for the diffusion time we can write $t_{D'} = d^2/D'$ which gives the characteristic frequency of eq 16. In the following we interpret our results based on the characteristic frequencies ω_β and $\omega_{D'}$. We assume $c \approx 3 \times 10^8$ m/s, $\alpha/\alpha' = 0.05$, $\alpha' = 10^6$ m^{-1}, and $S = c$ in all our calculations (note that these choices result in $\omega_\beta = \beta = 3 \times 10^{14}$ Hz). The calculations are then discussed based on the three independent variables in the problem, that is, d, ϵ/β, and κ/ϵ.

Figure 2 shows the real and imaginary parts of transfer function $M(\omega)$, for $\kappa/\epsilon = 0$ (zero nonradiative loss), $d\alpha' = 5$, and $\epsilon/\beta = 10^{-2}$, 10^{-4}, and 10^{-6}. These ratios have been estimated based on eq 3, using the values for the density of states of the typical semiconductors. The characteristic frequencies introduced in eqs 15 and 16 are also indicated in the figure. Three regions can be distinguished in each subfigure. At the low frequency or static region, that is, $\omega \ll \omega_{D'}$, the system can completely follow the perturbation, and as predicted in eq 14, one has $M = M' \approx 1$. In contrast, at the high frequency region, $\omega \gg \omega_\beta$, the system cannot follow the ac perturbation

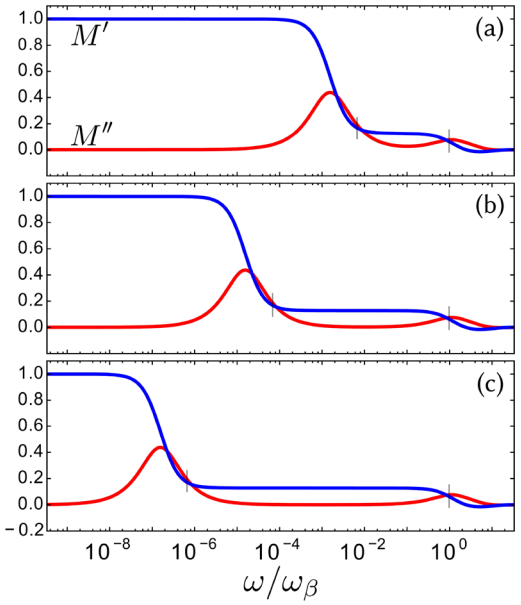

Figure 2. Real (M') and imaginary part (M'') of the transfer function M as a function of the normalized modulation frequency for $\kappa/\epsilon = 0$ and $d\alpha' = 5$, and different emission rate constants as $\epsilon/\beta = 10^{-2}$ (a), 10^{-4} (b), and 10^{-6} (c). Two characteristic frequencies of ω_β (high frequency feature) and $\omega_{D'}$ (low frequency feature), introduced in eqs 15 and 16, are shown for each case.

and therefore the response vanishes. There is also an intermediate region $\omega_{D'} < \omega < \omega_\beta$, where the system can partially respond to the perturbation. The most important feature in Figure 2 is that the plot can resolve the two characteristic frequencies of the problem. We return to this issue in Figure 4, where we discuss complex plane plot of the transfer function.

Figure 3 shows the transfer function for four different thickness d, and $\epsilon/\beta = 10^{-4}$. Characteristic frequency $\omega_{D'}$ is also indicated in each case. As can be seen, except for the case $d\alpha' \sim 1$ in which both $\omega_{D'}$ and ω_β are completely resolved (as in Figure 2), in the other cases, the transfer function shows a nonvanishing feature only near $\omega_{D'}$. This is because by increasing the thickness the time scale of the diffusion also increases and therefore very fast processes like absorption of the photons cannot be seen. For the same reason, as expected, by increasing the thickness, $\omega_{D'}$ shifts to the lower frequencies. The result of Figure 3 clearly shows that this is D' and not D that describes the photon diffusion process.

Now, we consider the effect of the nonradiative loss on the small perturbation response function. Figure 4 shows the results for $d\alpha' = 2$ and $\epsilon/\beta = 10^{-4}$, but with different nonradiative rates as $\kappa/\epsilon = 0$, 10^{-1}, 1, and 10^2 ($\equiv\infty$). For each case, we also show the complex plane plot of the transfer function [$M''(\omega)$ vs $M'(\omega)$]. In the case $\kappa/\epsilon = 0$, Figure 4a, since the thickness of the layer is not large (in comparison with $1/\alpha'$), both characteristic frequencies are resolved, and correspondingly, we have two distinct arcs in the complex plane plot. Note that in this case, $M(0) = 1$, see eq 14. However, by increasing κ, as shown in the right panel, the low-frequency part of the transfer function decays so finally in the case $\kappa \gg \epsilon$ it approaches to $M(0) \propto e^{-d\sqrt{\alpha\alpha'}}$. This is, in fact, the Beer–Lambert limit, as shown in eq 14. Correspondingly, the low-frequency arc in the complex plane disappears when $\kappa \gg \epsilon$. On the other hand, the high-frequency arc is independent

DOI: 10.1021/acs.jpclett.7b01563
J. Phys. Chem. Lett. 2017, 8, 3673−3677

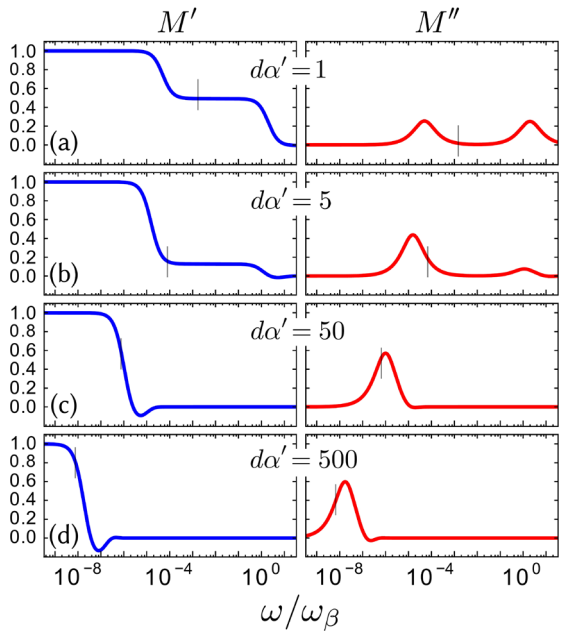

Figure 3. Real (M') and imaginary part (M'') of the transfer function M as a function of the normalized modulation frequency in the case of zero nonradiative loss $\kappa/\epsilon = 0$ and $\epsilon/\beta = 10^{-4}$, but four different thicknesses indicated in parts (a)–(d). Characteristic frequency $\omega_{D'}$, given by eq 16, is also indicated in each plot.

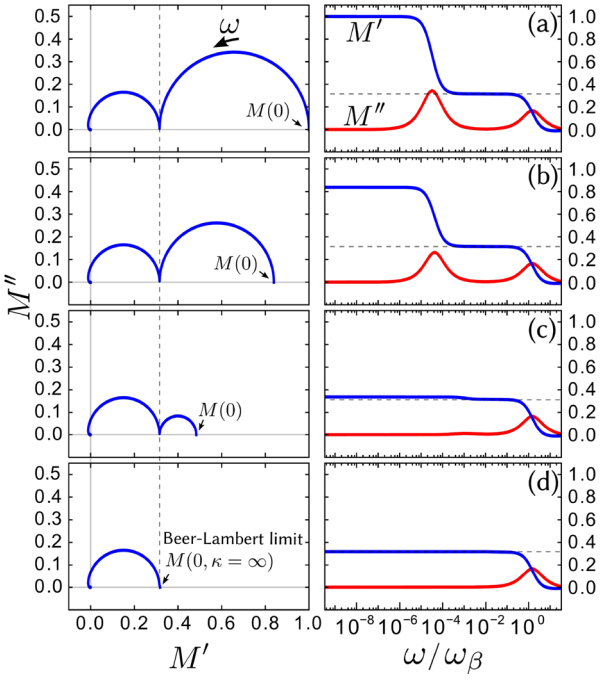

Figure 4. Effect of the nonradiative loss strength on the transfer function for $\kappa/\epsilon = 0$ (a), 10^{-1} (b), 1 (c), and 10^{2} (d) as a function of the normalized frequency (right), and corresponding complex plane plots (left). In all plots $\epsilon/\beta = 10^{-4}$ and $d\alpha' = 2$. $M(0)$, given by eq 14, is shown in each case. Dashed lines indicate response of the system if $\kappa \gg \epsilon$.

of the strength of the nonradiative loss, because it is only related to the absorption process. Another important feature in Figure 4 is that in the intermediate frequency range $\omega_{D'} < \omega < \omega_{\beta}$, the system responds as obeying the Beer–Lambert law, independent of the ratio κ/ϵ. In this regime, change in the incoming flux is fast enough to blur the fluorescence properties of the system.

In summary, we have introduced a new class of light-to-light transfer function, for the technique of light-modulated emission spectroscopy (LIMES) which can provide important information about the absorption/emission properties of an absorbing material. We showed how using the small perturbation frequency domain technique resolves time constants of the optical phenomena in an absorbing layer. Based on the trap-limited diffusion concept, we have provided a simple and intuitive picture for the photon transport in an absorbing layer. The photon absorption, photon annihilation/emission, and photon recycling have been explicitly included in our model. Importantly, by considering the probability of fluorescence emission, we found a general expression for the normalized intensity of a photon flux passing through an absorbing layer, which goes beyond the traditional Beer–Lambert law. This finding has important consequences on the interpretation of the experimental results usually used to find the absorption properties of the absorbing materials.

■ ASSOCIATED CONTENT

Supporting Information

The Supporting Information is available free of charge on the ACS Publications website at DOI: 10.1021/acs.jpclett.7b01563.

Transfer function for the photons generated due to Stoke's shift (PDF).

■ AUTHOR INFORMATION

Corresponding Authors

*E-mail: ansari.rad@shahroodut.ac.ir.

*E-mail: bisquert@uji.es.

ORCID

Mehdi Ansari-Rad: 0000-0003-3971-2251

Juan Bisquert: 0000-0003-4987-4887

Notes

The authors declare no competing financial interest.

■ ACKNOWLEDGMENTS

We acknowledge funding from MINECO of Spain under Project MAT2016-76892-C3-1-R and Generalitat Valenciana Project PROMETEOII/2014/020.

■ REFERENCES

(1) Fabregat-Santiago, F.; Garcia-Belmonte, G.; Mora-Seró, I.; Bisquert, J. Characterization of nanostructured hybrid and organic solar cells by impedance spectroscopy. *Phys. Chem. Chem. Phys.* **2011**, *13*, 9083–9118.

(2) de Jongh, P. E.; Vanmaekelbergh, D. Trap-limited electronic transport in assemblies of nanometer-size TiO_2 Particles. *Phys. Rev. Lett.* **1996**, *77*, 3427–3430.

(3) Huang, S. Y.; Schlichthörl, G.; Nozik, A. J.; Grätzel, M.; Frank, A. J. Charge recombination in dye-sensitized nanocrystallyne TiO_2 solar cells. *J. Phys. Chem. B* **1997**, *101*, 2576–2582.

(4) Fisher, A. C.; Peter, L. M.; Ponomarev, E. A.; Walker, A. B.; Wijayantha, K. G. U. Intensity dependence of the back reaction and transport of electrons in dye-sensitized nanocrystalline TiO_2 solar cells. *J. Phys. Chem. B* **2000**, *104*, 949–958.

(5) Bertoluzzi, L.; Bisquert, J. Investigating the consistency of models for water splitting systems by light and voltage modulated techniques. *J. Phys. Chem. Lett.* **2017**, *8*, 172–180.

(6) Gratton, E. Multifrequency phase and modulation fluorometry. *Annu. Rev. Biophys. Biomol. Struct.* **1984**, *13*, 105–124.

DOI: 10.1021/acs.jpclett.7b01563
J. Phys. Chem. Lett. 2017, 8, 3673–3677

(7) Chouffot, R.; Brezard-Oudot, A.; Kleider, J. P.; Brüggemann, R.; Labrune, M.; Roca i Cabarrocas, P.; Ribeyron, P. J. Modulated photoluminescence as an effective lifetime measurement method: Application to a-Si:H/c-Si heterojunction solar cells. *Mater. Sci. Eng., B* **2009**, *159−160*, 186−189.
(8) Wang, Q.; Ito, S.; Grätzel, M.; Fabregat-Santiago, F.; Mora-Seró, I.; Bisquert, J.; Bessho, T.; Imai, H. Characteristics of high efficiency dye-sensitized solar cells. *J. Phys. Chem. B* **2006**, *110*, 19406−19411.
(9) Bisquert, J. Beyond the quasi-static approximation: Impedance and capacitance of an exponential distribution of traps. *Phys. Rev. B: Condens. Matter Mater. Phys.* **2008**, *77*, 235203.
(10) Meyer, T. J. J.; Markvart, T. The chemical potential of light in fluorescent solar collectors. *J. Appl. Phys.* **2009**, *105*, 063110.
(11) Klimov, V. I.; Baker, T. A.; Lim, J.; Velizhanin, K. A.; McDaniel, H. Quality factor of luminescent solar concentrators and practical concentration limits attainable with semiconductor quantum dots. *ACS Photonics* **2016**, *3*, 1138−1148.
(12) Miller, O. D.; Yablonovitch, E.; Kurtz, S. R. Strong internal and external fluorescence as solar cells approach the Shockley-Queisser limit. *IEEE J. Photov.* **2012**, *2*, 303−311.
(13) Pazos-Outón, L. M.; Szumilo, M.; Lamboll, R.; Richter, J. M.; Crespo-Quesada, M.; Abdi-Jalebi, M.; Beeson, H. J.; Vrućinić, M.; Alsari, M.; Snaith, H. J.; Ehrler, B.; Friend, R. H.; Deschler, F. Photon recycling in lead iodide perovskite solar cells. *Science* **2016**, *351*, 1430−1433.
(14) Kirchartz, T.; Staub, F.; Rau, U. Impact of photon recycling on the open-circuit voltage of metal halide perovskite solar cells. *ACS Energy Lett.* **2016**, *1*, 731−739.
(15) Kittidachachan, P.; Danos, L.; Meyer, T. J. J.; Alderman, N.; Markvart, T. Photon collection efficiency of fluorescent solar collectors. *Chimia* **2007**, *61*, 780−786.
(16) Van Sark, W. G.; Barnham, K. W.; Slooff, L. H.; Chatten, A. J.; Büchtemann, A.; Meyer, A.; Mc.Cormack, S. J.; Koole, R.; Farrell, D. J.; Bose, R.; Bende, E. E.; Burgers, A. R.; Budel, T.; Quilitz, J.; Kennedy, M.; Meyer, T.; Wadman, S. H.; van Klink, G. P.; van Koten, G.; Meijerink, A.; Vanmaekelbergh, D. Luminescent Solar Concentrators. A review of recent results. *Opt. Express* **2008**, *16*, 21773−21792.

DOI: 10.1021/acs.jpclett.7b01563
J. Phys. Chem. Lett. 2017, 8, 3673−3677